



**HAL**  
open science

## Observation and analysis of $\nu_1 + \nu_3$ and $\nu_1 + 2\nu_4$ bands of CF<sub>4</sub> molecule

I.S. Chizhmakova, A.V. Nikitin, L.N. Sinitsa, V.I. Serdyukov, A.A. Lugovskoi,  
Michael M. Rey, Vladimir G. Tyuterev

► **To cite this version:**

I.S. Chizhmakova, A.V. Nikitin, L.N. Sinitsa, V.I. Serdyukov, A.A. Lugovskoi, et al.. Observation and analysis of  $\nu_1 + \nu_3$  and  $\nu_1 + 2\nu_4$  bands of CF<sub>4</sub> molecule. *Journal of Quantitative Spectroscopy and Radiative Transfer*, 2023, 306, pp.108616. 10.1016/j.jqsrt.2023.108616 . hal-04283799

**HAL Id: hal-04283799**

**<https://hal.science/hal-04283799>**

Submitted on 14 Nov 2023

**HAL** is a multi-disciplinary open access archive for the deposit and dissemination of scientific research documents, whether they are published or not. The documents may come from teaching and research institutions in France or abroad, or from public or private research centers.

L'archive ouverte pluridisciplinaire **HAL**, est destinée au dépôt et à la diffusion de documents scientifiques de niveau recherche, publiés ou non, émanant des établissements d'enseignement et de recherche français ou étrangers, des laboratoires publics ou privés.

## 1 **Observation and analysis of $\nu_1 + \nu_3$ and $\nu_1 + 2\nu_4$ bands of $\text{CF}_4$ molecule**

2  
3 I. S. Chizhmakova<sup>a</sup>, L. N. Sinitsa<sup>c</sup>, V. I. Serdyukov<sup>c</sup>, A. A. Lugovskoi<sup>c</sup>, M. Mattoussi<sup>d</sup>, M. Rey<sup>d</sup>, A. V.  
4 Nikitin<sup>b</sup>, and V. G. Tyuterev<sup>b,d</sup>

5  
6 *a Laboratory of Quantum Mechanics of Molecules and Radiative Processes, Tomsk State*  
7 *University, 36 Lenin Avenue, 634050 Tomsk, Russia*

8 *b Laboratory of Theoretical Spectroscopy, Institute of Atmospheric Optics, Russian Academy*  
9 *of Sciences, 634055 Tomsk, Russia*

10 *c Laboratory of Molecular Spectroscopy, Institute of Atmospheric Optics, Russian Academy*  
11 *of Sciences, 634055 Tomsk, Russia*

12 *d GSMA, UMR CNRS 7331, University of Reims Champagne Ardenne, Moulin de la Housse*  
13 *B.P. 1039, F-51687, Cedex Reims, France*

### 14 15 **Abstract**

16 Infrared spectra of  $\text{CF}_4$  molecule were measured for three different temperatures in the  
17 range 2160–2210  $\text{cm}^{-1}$  using Fourier transform spectrometer. Non-empirical effective  
18 Hamiltonian obtained from the potential energy surface using the contact transformation  
19 method was used for the modeling of line positions. The origins of two bands  $\nu_1 + \nu_3$  ( $\text{F}_2$ ) and  
20  $\nu_1 + 2\nu_4$  ( $\text{F}_2$ ) at 2186.97 and 2168.21  $\text{cm}^{-1}$  were experimentally determined for the first time.  
21 The experimental origin of the weak  $\nu_1 + 2\nu_4$  ( $\text{E}$ ) sub-band was tentatively evaluated near  
22 2169.84  $\text{cm}^{-1}$ . Ab initio line intensities were calculated from high order dipole moment  
23 surface by variational method using the TENSOR computational code in the normal mode  
24 representation. The analyses of experimental spectra were carried out using the MIRS  
25 program suite accounting for the full tetrahedral symmetry of the molecule.

26  
27 **Key words:** Carbon tetrafluoride,  $\text{CF}_4$ , ab initio, analysis spectra, intensities, position  
28  
29  
30  
31  
32  
33  
34

## 35 Introduction

36

37 Tetrafluoromethane (CF<sub>4</sub>), also known as Halocarbon 14, PFC-14 or R-14 etc., is a  
38 colorless, non-toxic, non-flammable, non-corrosive gas belonging to the family of  
39 perfluorocarbons (PFCs). The concentration of the carbon tetrafluoride in the troposphere is  
40 low [1] [2] [3], however its growth in recent decades has been associated with industrial  
41 blowouts, the most significant of which is the production of aluminum [4].

42 Recently, the amount of CF<sub>4</sub> in the Earth's atmosphere has increased, and its lifetime  
43 in the atmosphere could reach 50 thousand years according to evaluations of Ref. [5]. This is  
44 because CF<sub>4</sub> molecules, compared to other freons, are not chemically active that leads to their  
45 accumulation in the atmosphere. CF<sub>4</sub> is a highly absorbing molecule in the infrared range and  
46 has one of the largest known global warming potentials (GWP) [6]. Consequently,  
47 tetrafluoromethane can play an active role in global climate change and falls under the  
48 directives of Kyoto Protocol of the United Nations Framework Convention on Climate  
49 Change (UNFCCC) for species recommended for environmental monitoring [2] [3] [7].

50 To determine the concentration of CF<sub>4</sub> in the atmosphere related to above mentioned  
51 climatic issues, it is necessary to compare remote measurements of the absorption function  
52 with the spectra obtained by the modeling of laboratory experiments at various temperature  
53 conditions. To this end, it is necessary to make an accurate calculation of frequencies and  
54 intensities, accounting for the selection rules for absorption lines, which strongly depend on  
55 the symmetry of the molecule.

56 CF<sub>4</sub> molecule belongs to the tetrahedral T<sub>d</sub> point group, like methane, but it is heavier  
57 than CH<sub>4</sub>. It has thus lower vibrational modes and rotational levels populated at higher J  
58 quantum numbers, even at room temperature. The spectra of this molecule are characterized  
59 by the presence of complex Fermi resonance interactions, which significantly complicates the  
60 description of their vibrational-rotational patterns. The spectra of the CF<sub>4</sub> molecule have been  
61 studied over the past decades both theoretically and experimentally [8] [9] [10] [11].  
62 However, currently available versions of databases such as HITRAN [12] [13] and GIESA  
63 [14] [15], include information for strong bands only.

64 The purpose of this work is to analyze the strong band  $\nu_1 + \nu_3$  as well as the nearby  
65 band  $\nu_1 + 2\nu_4$ , which are coupled by strong interactions. These bands are part of the 9-th  
66 polyad (heptad) of CF<sub>4</sub>, containing seven bands in the spectral range 2120–2260 cm<sup>-1</sup>. These  
67 seven bands correspond to unevenly localized upper state vibrational levels, as shown in  
68 figure 1. The weak band  $2\nu_2 + 2\nu_4$  having ten upper state vibrational sublevels

69 ( $A_1, A_2, 2F_1, 3F_2, 3E$ ) is localized near  $2130 \text{ cm}^{-1}$ . The band  $2\nu_2 + \nu_3$  has three upper state  
70 vibrational sublevels ( $F_1, 2F_2$ ). The corresponding transitions to one of two  $F_2$  sublevels are  
71 well identified in experimental spectra. The resonance interaction of  $2\nu_2 + \nu_3$  with  $\nu_1 + \nu_3$  is  
72 less pronounced compared to the coupling  $\nu_1 + 2\nu_4 / \nu_1 + \nu_3$ . The strong  $\nu_1 + \nu_3$  band has  
73 only one upper state vibrational levels ( $F_2$ ), whereas the  $\nu_1 + 2\nu_4$  has three vibrational sub-  
74 levels ( $A_1, F_2, E$ ). Both bands investigated in this work lie near the  $5\nu_2$  ( $A_1, A_2, E$ ) sub-bands,  
75 but the corresponding perturbations were not found. Another two bands  $\nu_1 + 3\nu_2$  with  
76 ( $A_1, A_2, E$ ) upper state sublevels and  $2\nu_1 + \nu_2$  ( $E$ ) are located at the upper edge of the polyad.

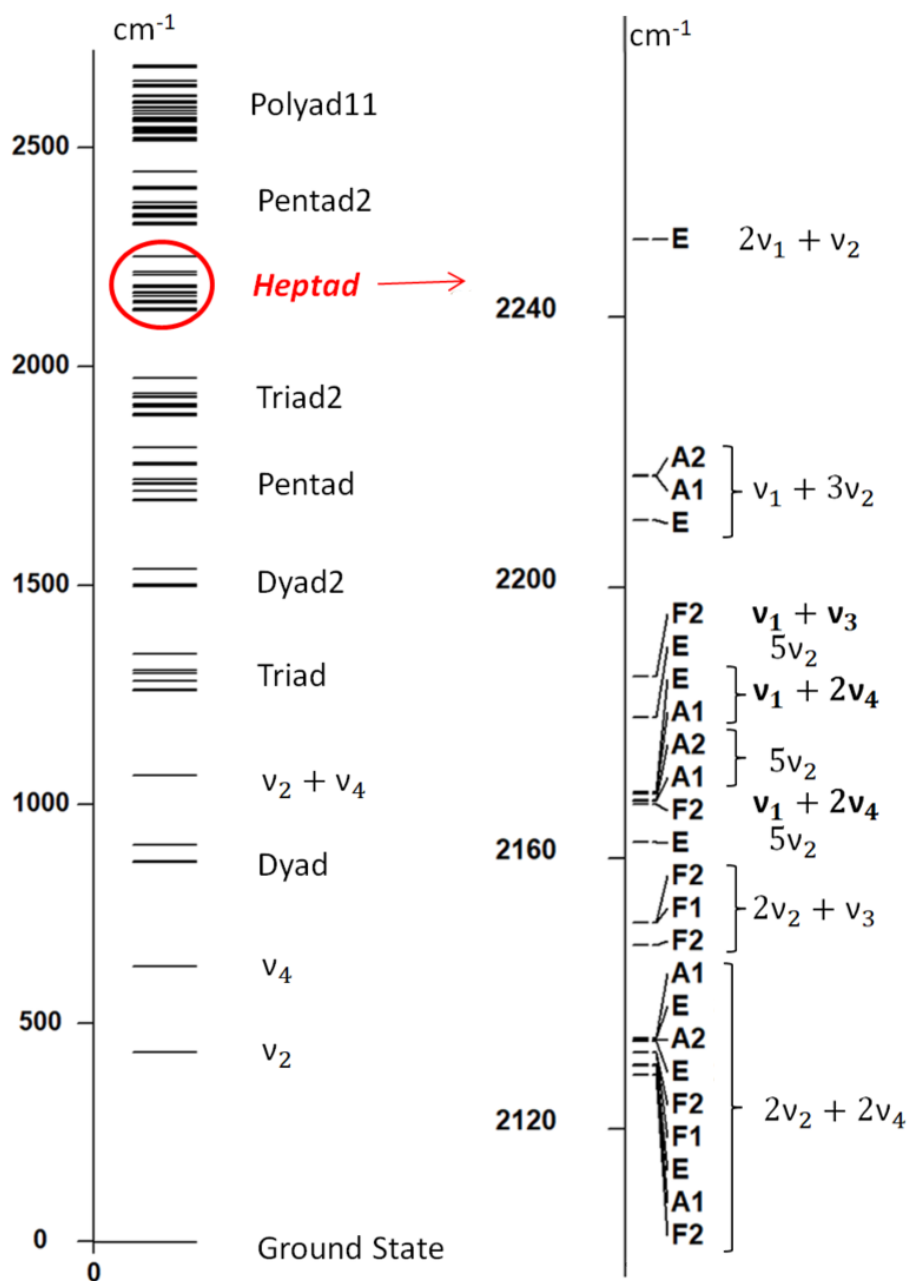
77 The analyses of experimental spectra were carried out using the MIRS program suite  
78 [16] [17] accounting for the full symmetry of the molecule using tetrahedral tensorial  
79 formalism [18] [19].

80 Similarly to our previous work [20], we applied a mixed approach involving an  
81 Effective Hamiltonian (EH) model obtained from the ab initio potential energy surface (PES)  
82 using high-order contact transformations (CT) [21], [22], [23]. An alternative version of  
83 numerical transformations from PES to EH is presented in the work [24].

84 To construct an ab initio line list of  $\text{CF}_4$  we used the potential energy surfaces and the  
85 dipole moment surfaces (DMS), which were described in detail in [11]. This work is part of  
86 the TheoReTS project [25], devoted to the development of complete theoretical line lists for  
87 polyatomic molecules based on ab initio PESs and DMSs.

88 For experimental study of the spectra of greenhouse gases at low temperatures, single-  
89 and multi-pass low-temperature cells have been created in the Institute of Atmospheric Optics  
90 in Tomsk. The theoretical line lists obtained in this work were validated with success by a  
91 direct comparison with the infrared Fourier spectra recorded at  $T = 113 \text{ K}$  and  $T = 296 \text{ K}$  in  
92 the region of  $2160\text{--}2210 \text{ cm}^{-1}$ .

93



94

95

96 **Figure1.** Scheme of vibrational polyads of the  $\text{CF}_4$  molecule (left) and vibrational sublevels  
 97 of the hexad (right). The states investigated in this work are distinguished by boldface script.

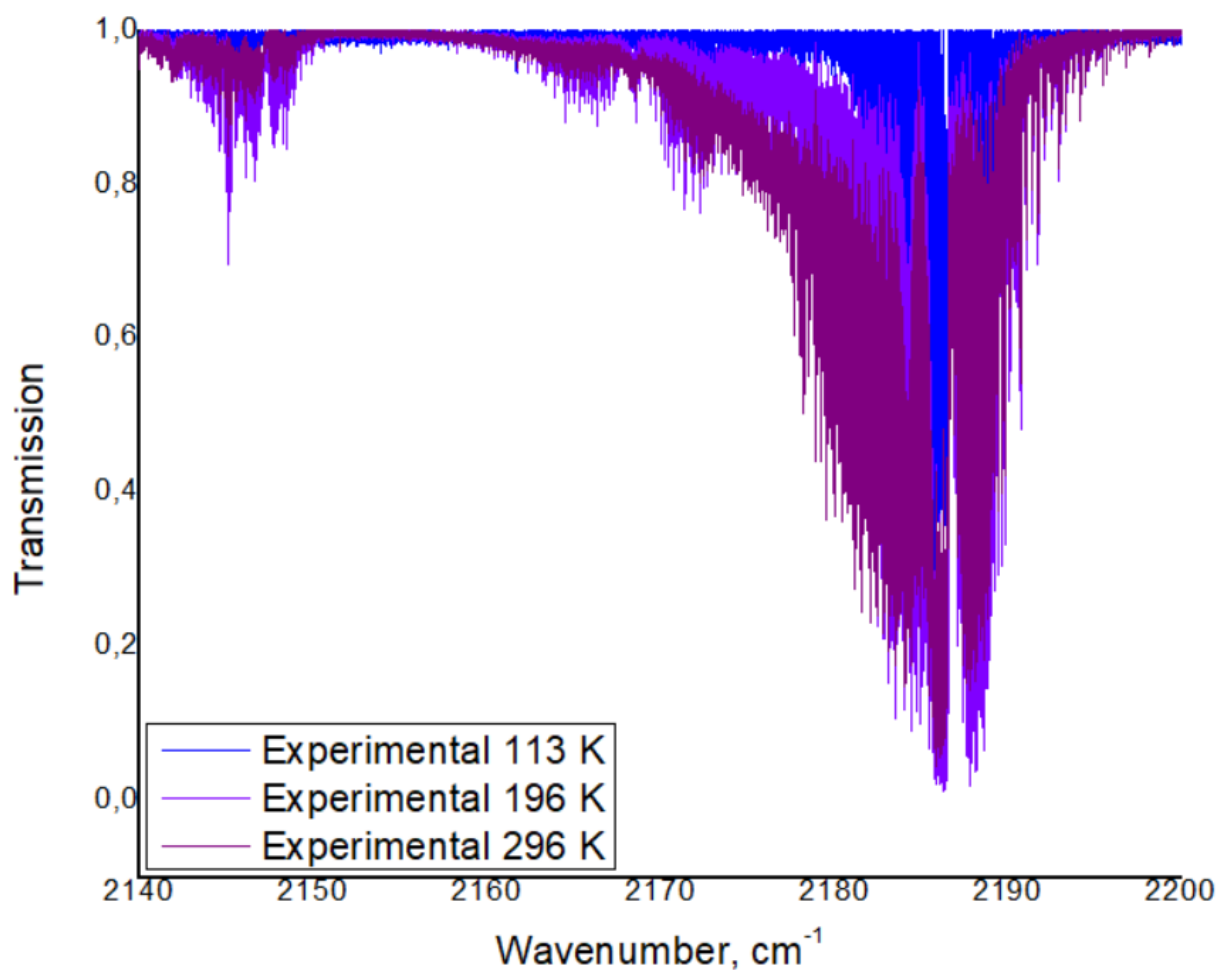
98

99 Experimental spectra recorded in this work are described in Section 2. Section 3 gives  
 100 an overview of the theoretical model for tetrahedral molecules used for our analysis. The last  
 101 Section 4 contains the conclusions and discussions of the results.

102

103 **2 Experiment**

104 The absorption spectra of carbon tetrafluoride were recorded using a Bruker IFS 125-  
105 M Fourier spectrometer with two single-pass cells. The first cell, 220 cm long, with windows  
106 made of ZnSe and KBr and the possibility of cooling by liquid alcohol, was used to record  
107 spectra at room temperature and the temperature of 196 K. The second cell, 20 cm long,  
108 cooled with liquid nitrogen was used to record spectra at the temperature of 113 K. In total,  
109 the spectra were recorded for three temperatures 296, 196 and 113 K. In the range 2160–2210  
110  $\text{cm}^{-1}$   $\text{CF}_4$  has strong absorption bands with line intensities up to  $10^{-21} \text{ cm}^{-1}/\text{molecule} \times \text{cm}^{-2}$ .  
111 The MIR globe was used as the radiation source, the beam splitter was made of  $\text{CaF}_2$ , and an  
112 MST cooled with liquid nitrogen was used as a photodetector. Pressure measurements were  
113 made by an AIR-20 M pressure sensor with a pressure measurement range of 0–100 kPa and  
114 an accuracy of about 0,1%. The temperature stabilization in the measurement room with a  
115 volume of  $75 \text{ m}^3$  was carried out using a Midea MSE-24HR air conditioner with an error of  
116 less than 1 K that allowed for long time measurements. The radiation after the cell was  
117 introduced into the Fourier spectrometer through the radiation channel. The spectrometer was  
118 not evacuated, so the recorded spectra show strong water vapor lines broadened by air  
119 pressure at one atmosphere. The 113 K spectrum was calibrated using four lines 2114.4255,  
120 2115.0160, 2136.1433, 2161.7255  $\text{cm}^{-1}$ . Calibration of the spectra for temperatures of 296 K  
121 and 196 K was made according to the positions of several  $\text{CF}_4$  transitions obtained from the  
122 113 K spectrum. All spectra were recorded with a spectral resolution of  $0,005 \text{ cm}^{-1}$  (Table 1)  
123 using the diaphragm with the diameter of 1.1 mm. 350 scans were recorded with a scanner  
124 position measurement frequency of 20 kHz. The pressure was measured at room temperature  
125 to give 1.6775 and 6.7 mbar for the spectra with an optical path length of 220 and 20 cm,  
126 respectively. The signal-to-noise ratio in the recorded spectra was about 1000 in the  
127 measurement region. The uncertainty of the pressure measurements at low temperatures  
128 inside the cell significantly contributed to the errors of line intensity determination. The total  
129 error of the line intensities measurements did not exceed 10%. The experimental spectra  
130 recorded in the specified range are shown in Figure 2. Note that only the bands  $\nu_1 + \nu_3$ ,  $\nu_1 +$   
131  $2\nu_4$ ,  $2\nu_2 + \nu_3$  and  $5\nu_2$  fall within the range of our experiment. The spectra at a temperature of  
132 113 K contain several water absorption features.



133

134 **Figure 2.** Transmittance spectrum of CF<sub>4</sub>, recorded at temperatures 296 K (black), 196 K  
 135 (magenta) and 113 (blue) K in the spectral range between 2130 and 2200 cm<sup>-1</sup>.

136

137 **Table 1.** Experimental details

Spectra Range (cm <sup>-1</sup> )	2137-2205	2112-2205
Resolution (cm <sup>-1</sup> )	0.005	0.005
Source	Globar	Globar
Separator	CaF <sub>2</sub>	CaF <sub>2</sub>
Detector	MCT	MCT
Cell	220cm low temperature vacuum cell	20cm low temperature vacuum cell
Optical Path (cm)	220	20
Temperatures K	296±2, 196±2	113±4
Initial Pressure (mbar) at 296K	1.775±0.0025	6.7±0.002
Aperture Diameter (mm)	1.1	1.1

### 3. Theoretical modeling of the observed spectrum in the range 2160 – 2210 cm<sup>-1</sup>

Despite a significant progress in the construction of accurate ab initio PESs and DMSs and in variational calculations for band origins and line intensities, the bands under study have not been identified in experimental spectra so far. Due to its high tetrahedral symmetry, CF<sub>4</sub> exhibits degenerate normal modes of vibration while the closely lying rovibrational levels are grouped into so-called polyads, leading to strong and complex resonance interactions. A well-known difficulty in purely empirical effective models is that the parameters of the resonance interactions may be ambiguously determined from the least-square fits [23] [26]. In this work, a non-empirical effective Hamiltonian - initially derived in [20] - was constructed from the optimized ab initio PES [11] by applying high-order contact transformations (CT) [21], [22] [23] [24] and was used in the analyses. This approach allowed us to calculate resonance parameters fairly accurately, which significantly simplifies the process of fitting parameters compared to purely empirical models [23]. A detailed description of ab initio calculations of potential energy and dipole moment surfaces, as well as global variational calculations is given in [11].

The MIRS computational code [16] was used to obtain the parameters of the effective Hamiltonian in the same way as it was described in previous papers to fully account for the properties of the tetrahedral symmetry of the molecule. Then these parameters were refined by a fine tuning using the fit to experimental line positions and CF<sub>4</sub> energy levels.

In this paper, transitions from the ground state (GS) to the states  $\nu_1 + \nu_3$ ,  $\nu_1 + 2\nu_4$  and  $2\nu_2 + \nu_3$  of the Heptad (9th polyad) are investigated. The effective vibration-rotation Hamiltonian adapted to the polyad structure of CF<sub>4</sub> is expressed as follows:

$$H = \sum H_k = \tilde{H}_{P_0} + \tilde{H}_{\nu_2} + \tilde{H}_{\nu_4} + \tilde{H}_{Dyad} + \tilde{H}_{\nu_2+\nu_4} + \tilde{H}_{Tetrad} + \tilde{H}_{Dyad2} + \tilde{H}_{Pentad} \\ + \tilde{H}_{Heptad} + \tilde{H}_{Pentad2} + \tilde{H}_{Polyad11}$$

A comparison of the band origins obtained using the high-order CT method with previously determined experimental values of CF<sub>4</sub> was given in Table 11 and Figure 9 of ref [11]. The RMS deviation between variational [11] and CT calculations [20] using the same PES was very small, about 0.003 cm<sup>-1</sup> in the range 0–2700 cm<sup>-1</sup>. This allowed us to safely use the corresponding mixed ab initio / effective approach to analyses the observed spectra.



170 A schematic representation of the polyad structure as well as the scheme of vibrational  
 171 levels for tetrafluoromethane is shown in Figure 1. The enlarged scale on the right-hand side  
 172 represents the vibrational sublevels and their symmetry types in the range under  
 173 consideration. At the first stage, the centers of the two strongest bands were adjusted using  
 174 several observed transitions. This made it possible to significantly improve the calculated  
 175 positions of most transitions in the spectral range 2160–2205 cm<sup>-1</sup>.

176 At the second stage, we determined the line intensities. The infrared spectra of CF<sub>4</sub> are  
 177 very dense due to the large number of transitions belonging to both cold and hot bands that  
 178 significantly complicates the analysis of experimental spectra. The variational method using  
 179 the ab initio DMS [11] made it possible to accurately determine line intensities from first  
 180 principles calculations. Consequently, we adjusted the parameters of the effective dipole  
 181 moment (EDM) directly to the variational intensities calculated in [11]. This approach has  
 182 already been successfully applied in our previous work [20]. The obtained EDM parameters  
 183 are shown in Table 2. As a result, a good agreement between the variational and experimental  
 184 intensity of the lines, was achieved (achieved) as shown in Figure 5.

185

186 [Table 2. Effective dipole transition moment parameters for the  \$\nu\_1 + \nu\_3\$ ,  \$\nu\_1 + 2\nu\_4\$  and  \$2\nu\_2 +\$   
 187  \$\nu\_3\$  bands](#)

Torsorial nomenclature			Parameter value
	Rotational	Vibrational	
1	9 R 0( 0, 0A1)	0000 0210	3.0677673220E-04
2	9 R 0( 0, 0A1)	0000 0210	-7.0097729574E-05
3	9 R 0( 0, 0A1)	0000 1002	-0.5582053784E-04
4	9 R 0( 0, 0A1)	0000 1010	7.4121145986E-03
5	9 R 1( 1, 0F1)	0000 1002	-8.0011070683E-06
6	9 R 1( 1, 0F1)	0000 1010	1.3437943401E-07
7	9 R 2( 0, 0A1)	0000 1010	9.8005076990E-09
8	9 R 2( 2, 0E )	0000 1010	1.8003881577E-08
9	9 R 2( 2, 0F2)	0000 1010	-3.0670244770E-08

188

189 At the third stage, a more detailed optimization of the effective Hamiltonian using the  
 190 observed transitions was made.

191

192

193

194

195

196

197 Table 3. Bands origins and integrated band intensities

Sub-bands	band origins computed [11], [24] from the PES, $\text{cm}^{-1}$	Vibrational band centers, $\text{cm}^{-1}$ , TW	Integrated band intensity, $\text{cm} / \text{molecule}$
$2\nu_2 + 2\nu_4$ F <sub>2</sub>	2128.14	2128.129140	2.967E-21
$2\nu_2 + 2\nu_4$ A <sub>1</sub>	2129.41	2129.406546	
$2\nu_2 + 2\nu_4$ E	2129.67	2129.673834	
$2\nu_2 + 2\nu_4$ F <sub>1</sub>	2131.42	2131.412124	
$2\nu_2 + 2\nu_4$ F <sub>2</sub>	2131.46	2131.457598	
$2\nu_2 + 2\nu_4$ E	2133.07	2133.066099	
$2\nu_2 + 2\nu_4$ A <sub>2</sub>	2133.29	2133.291210	
$2\nu_2 + 2\nu_4$ E	2133.54	2133.538461	
$2\nu_2 + 2\nu_4$ A <sub>1</sub>	2133.59	2133.592973	
$2\nu_2 + \nu_3$ F <sub>2</sub>	2147.34	2147.263493	
$2\nu_2 + \nu_3$ F <sub>2</sub>	2150.65	2150.571641	-
$2\nu_2 + \nu_3$ F <sub>1</sub>	2150.60	2150.528037	1.620E-20
$5\nu_2$ E	2162.46	2162.464206	7.416E-22
$5\nu_2$ A <sub>1</sub>	2168.54	2168.546631	
$5\nu_2$ A <sub>2</sub>	2168.65	2168.653221	
$5\nu_2$ E	2180.86	2180.861649	
$\nu_1 + 2\nu_4$ F <sub>2</sub>	2168.21	2168.013546	5.620E-20
$\nu_1 + 2\nu_4$ A <sub>1</sub>	2169.55	2169.551443	4.243E-21
$\nu_1 + 2\nu_4$ E	2169.84	2169.836080	4.972E-20
$\nu_1 + \nu_3$ F <sub>2</sub>	2186.97	2186.871327	5.228E-19
$\nu_1 + 3\nu_2$ F <sub>2</sub>	2209.97	2209.974243	1.767E-21
$\nu_1 + 3\nu_2$ A <sub>2</sub>	2216.56	2216.559310	

198

199

200

201

202

203

204

205

206

207

208

209

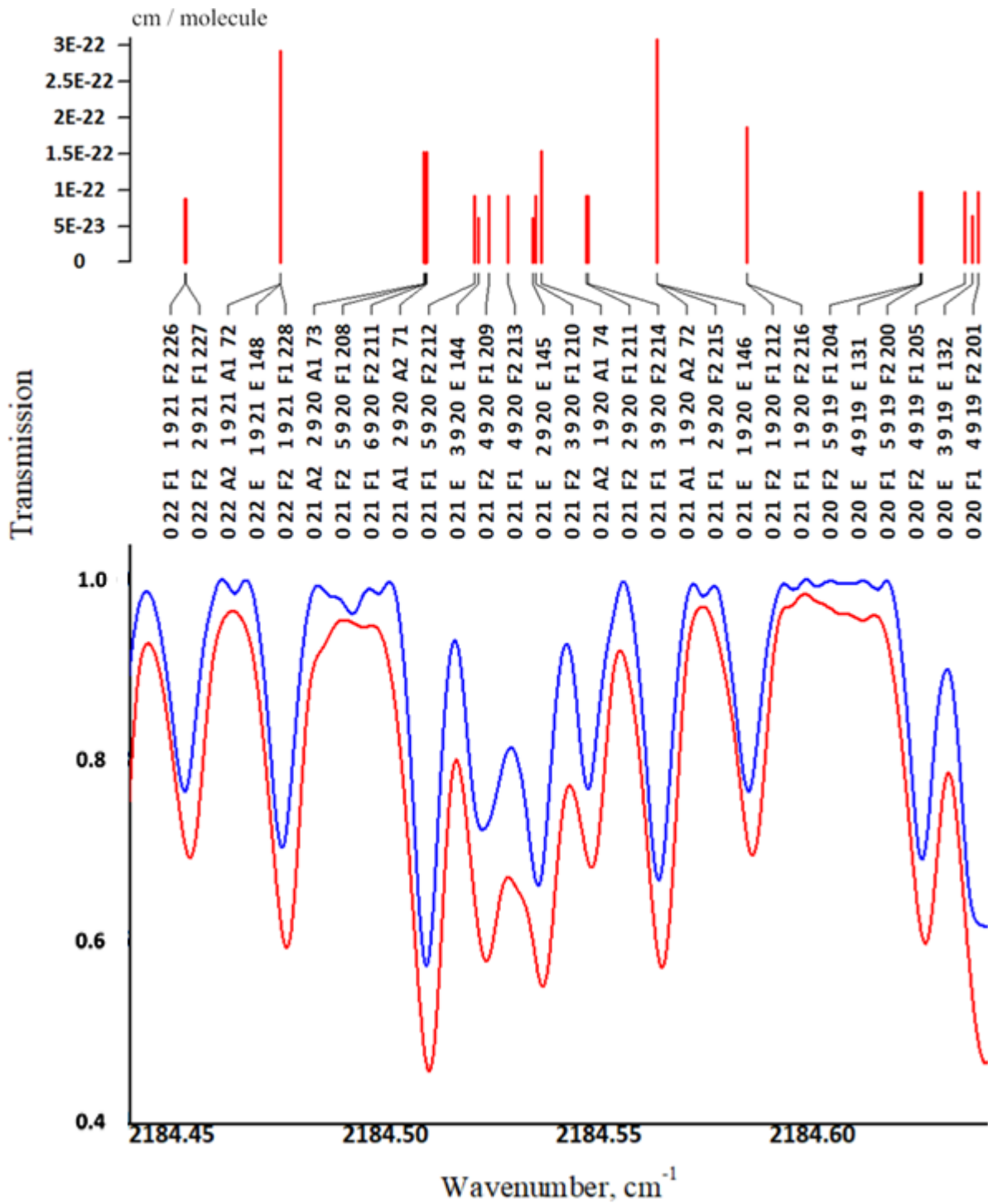
210

211

212

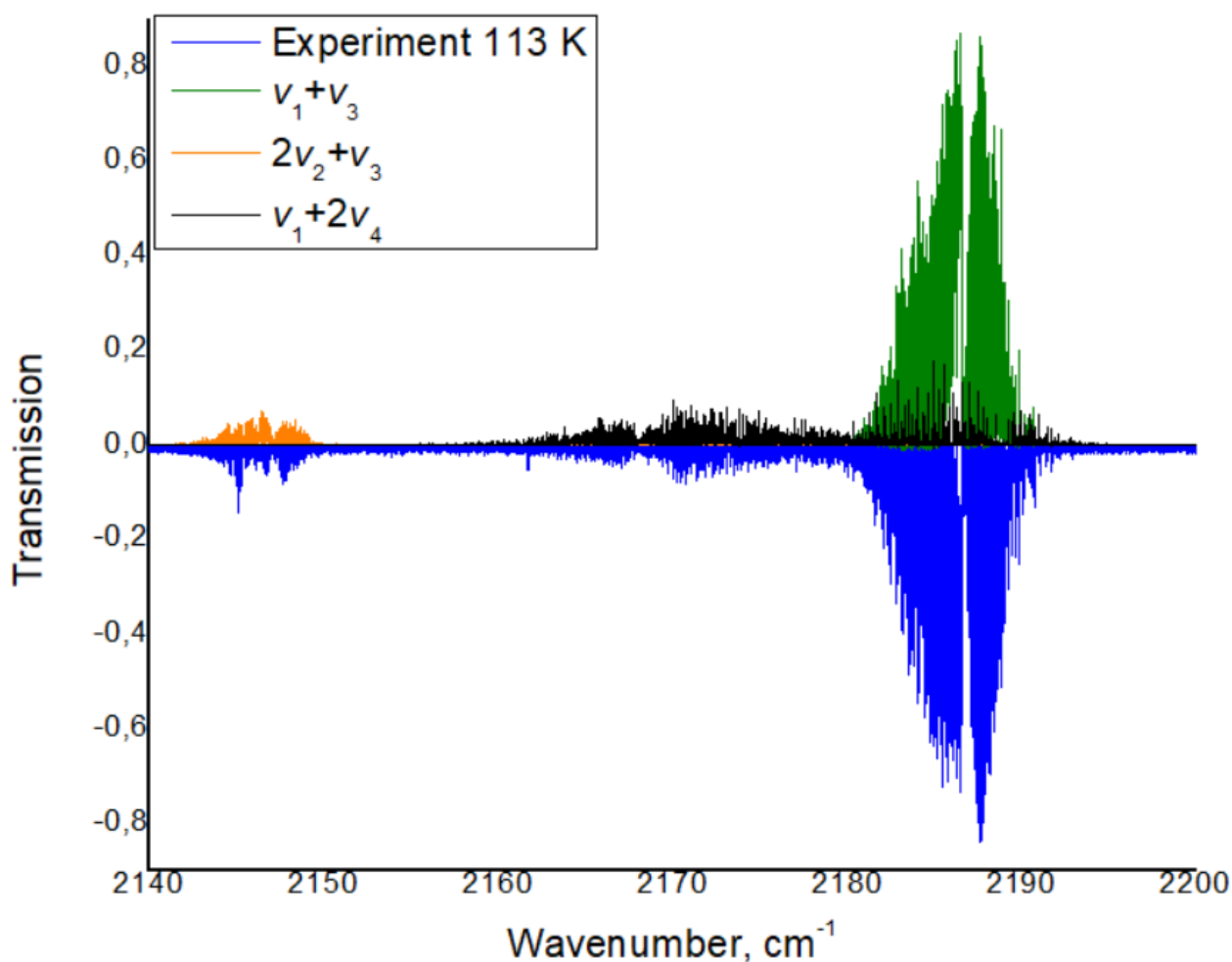
The complexity of the CF<sub>4</sub> spectra in the range 2137–2205  $\text{cm}^{-1}$  is due to overlapping cold and hot bands, including the transitions with three-, four-, and five vibrational quanta. Theoretical and experimentally determined band origin belonging to heptad band system are summarized in Table 3. The integrated intensities of cold bands given in the last columns of Table 3 correspond to ab initio calculations of ref [11]. The centers of the hot bands could not be accurately determined without a detailed analysis of the upper polyads. In addition, due to the high density of transitions, it was not possible to find the positions of individual lines. Instead, the spectra show peaks corresponding, at best, to a combination of strong transitions with certain values of the upper and lower J of one vibrational band. Similar sets of transitions were observed in the multiplets of the band  $2\nu_3$  (F<sub>2</sub>) of methane [27] [28]. In the case of methane many individual transitions in the multiplets could still be identified. However, in the case of the heavier CF<sub>4</sub> molecule, the spectra are much more crowded, and it was not possible to resolve individual transitions in this range. Most likely, it would be possible to identify individual transitions with  $J < 5$  at lower temperatures with longer optical paths, but at the

213 temperature of 113 K, the transitions with  $J < 5$  were noticeably weaker than the transitions  
214 with  $J = 10\text{--}20$  and, as a rule, were not visible. Either some multiplets of a band were blended  
215 by transitions of another bands, or the multiplets of one band with different  $J$  values  
216 overlapped each other. Such multiplets could not be used for assignments of individual lines.  
217 However, in many cases, the multiplets consisted of closely spaced transitions with the same  
218 values of  $J$ , and the center of the multiplet was determined quite accurately from the  
219 experiment. Several of these multiplets are shown in Figure 3.  
220



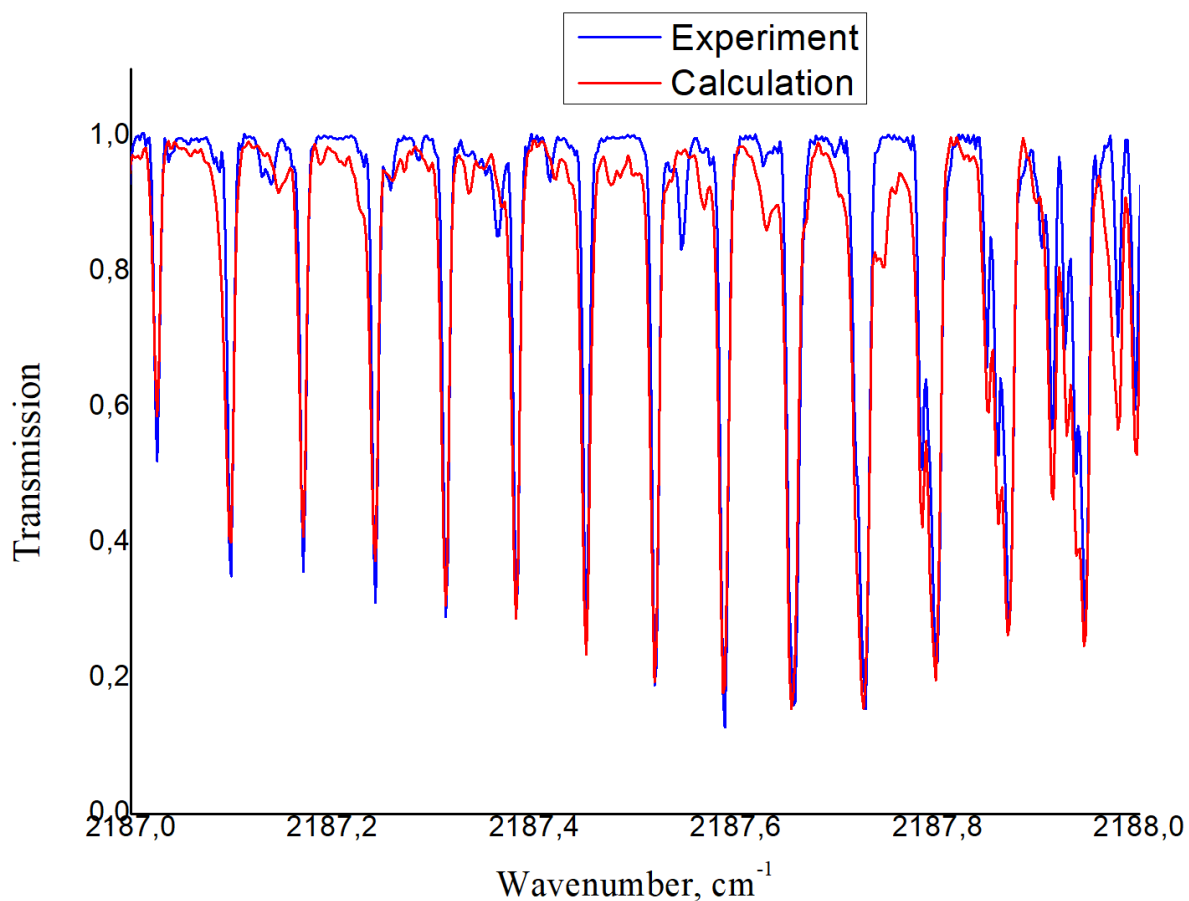
221  
222  
223  
224

**Figure 3.** Comparison of the simulated spectra with the measurements at  $T = 113$  K in the 2184.4–2184.7  $\text{cm}^{-1}$  region: upper panel –spectral lines from our line list at  $T = 113$  K (red); lower panel – observed spectra (blue) and simulations using our line list (red).



225  
 226 **Figure 4.** Comparison of the spectra simulations of CF<sub>4</sub> using our calculated line list with  
 227 measurements at  $T=113$  K in the  $2140.0-2200.0$  cm<sup>-1</sup> region: upper panel  $\nu_1+\nu_3$  (green),  
 228  $2\nu_2+\nu_3$  (black) and  $\nu_1+2\nu_4$  (orange); lower panel –experimental (blue) spectra  $T=113$  K.  
 229

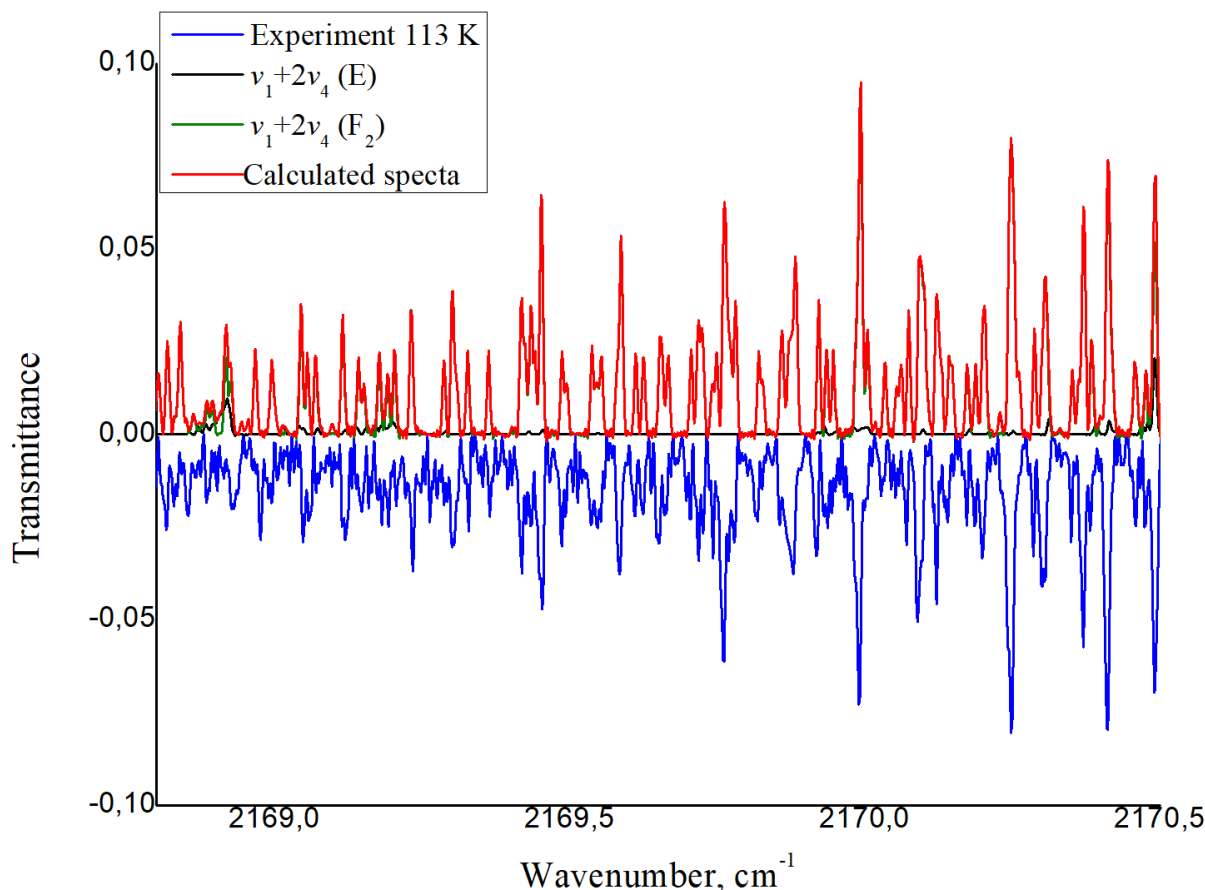
230 The strongest absorption in this range is due to the  $\nu_1 + \nu_3$  band with the integrated  
 231 intensity of more than  $5.2 \times 10^{-19}$  cm/molecule. The origin of this band predicted from the PES  
 232 [11] was  $2186.97$  cm<sup>-1</sup>. To fit the effective Hamiltonian, 284 multiplets were identified for the  
 233 R and P branches in the range  $2184.737-2188.023$  cm<sup>-1</sup> with  $J_{\max}=20$  and  $J_{\min}=4$ . Most of the  
 234 multiplets at the R and P branches were well separated from each other and their assignment  
 235 using ab initio predictions was often straightforward. A slight adjustment of the interaction  
 236 parameter between the upper states of  $\nu_1 + \nu_3$  and  $\nu_1 + 2\nu_4$  (F<sub>2</sub>) noticeably improved the  
 237 quality of fit for the positions of the strong  $\nu_1 + \nu_3$  band. Then, we tried to find some  
 238 assignments of weak band  $\nu_1 + 2\nu_4$  (F<sub>2</sub>) transitions.



239  
 240 **Figure 5.** Detailed comparisons of the transmission in experimental and simulated spectra of  
 241  $\text{CF}_4$  at 113 K in the R branch of  $\nu_1 + \nu_3$ .

242

243 The absorption of the  $\nu_1 + 2\nu_4$  band is five times weaker, with the ab initio estimation  
 244 of the integrated intensity of  $1.027 \times 10^{-19}$  cm/molecule. The transitions to the sublevel  $\nu_1 +$   
 245  $2\nu_4$  ( $F_2$ ) provide the largest contribution to the absorption for this band. However, an  
 246 assignment of transitions corresponding to this sublevel turned out to be much more difficult  
 247 than for  $\nu_1 + \nu_3$ . It was possible to find a good match only in the spectral range 2169.5–  
 248  $2170.5 \text{ cm}^{-1}$  (see Figure 6). In this range, the multiplets of the R branch are well visible in the  
 249 observed spectra for the upper state rotational quantum numbers  $J=7-19$ .

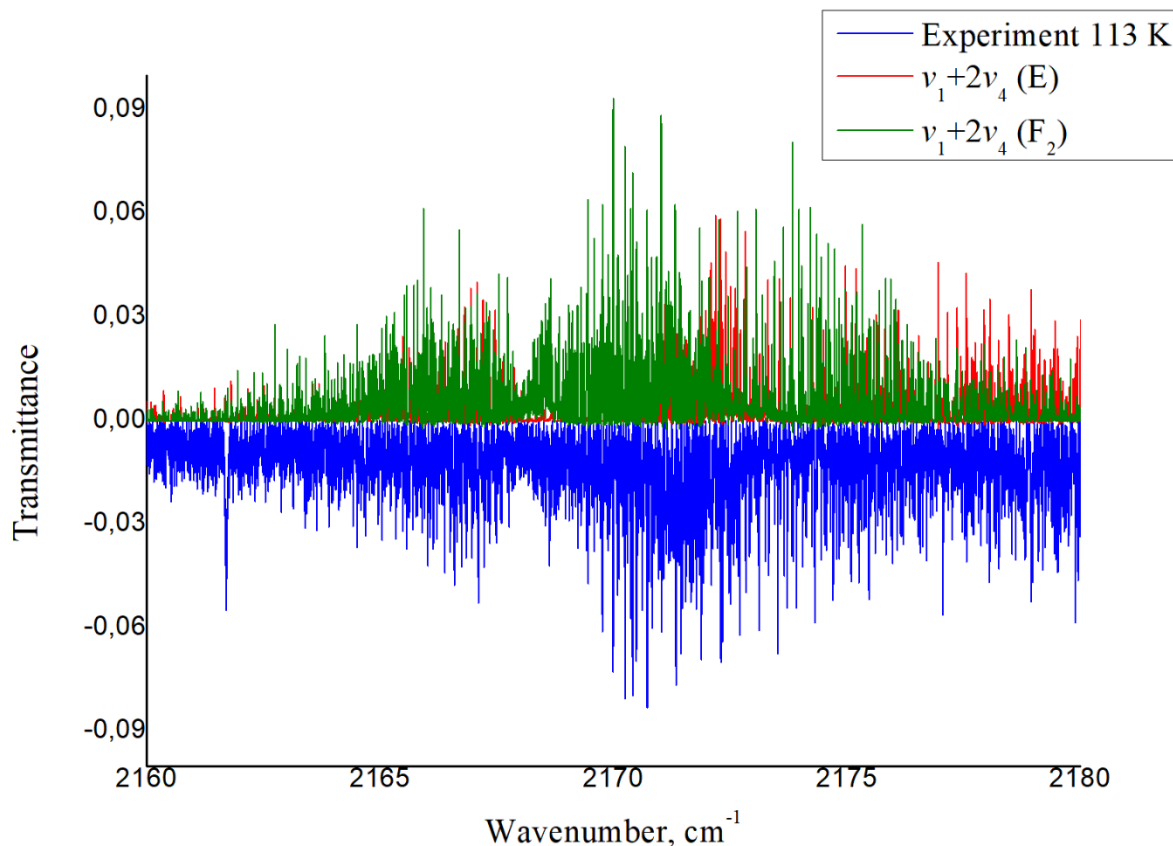


250  
 251 **Figure 6.** The comparison of simulated and observed spectra of CF<sub>4</sub> for  $T= 113$  K in the  
 252  $2169.8 - 2170.5$   $\text{cm}^{-1}$  region: calculated (red) spectra and  $\nu_1 + 2\nu_4$  (E) (black); lower panel –  
 253 experimental (blue) spectra  $T = 113$  K.  
 254

255 The center origin of  $\nu_1 + 2\nu_4$  (F<sub>2</sub>) was predicted from the PES at  $2168.21$   $\text{cm}^{-1}$  [11]. A  
 256 total of 117 multiplets for the R and P branches were identified to fit the effective  
 257 Hamiltonian in the range  $2169.0481 - 2170.4171$   $\text{cm}^{-1}$  with  $J_{\text{max}}= 19$  and  $J_{\text{min}}=7$ . Considering  
 258 that the levels with  $J < 7$  were not identified, the uncertainty of empirically determined band  
 259 origin was estimated as  $0,01$   $\text{cm}^{-1}$ . The identification of  $J \leq 7$  is a rather difficult task due to  
 260 the high density of lines in this range. After fitting the parameters of the effective Hamiltonian  
 261 to assigned transitions, the origins of the bands  $\nu_1 + \nu_3$  and  $\nu_1 + 2\nu_4$  (F<sub>2</sub>) were determined at  
 262  $2186.87$   $\text{cm}^{-1}$  and  $2168.007$   $\text{cm}^{-1}$  correspondingly. Note that the empirical values of some  
 263 sublevels of the F<sub>2</sub> symmetry of the heptad were slightly changed with respect to the previous  
 264 works, see Table 3.

265 Multiplets for the  $\nu_1 + 2\nu_4$  (E) sub-band could not be identified, because of the  
 266 weakness of the corresponding transitions compared to  $\nu_1 + 2\nu_4$  (F<sub>2</sub>), see Figure 7. The value  
 267 of the vibrational  $\nu_1 + 2\nu_4$  (E) sublevel did not change ( $2169.836$   $\text{cm}^{-1}$ ), but the positions of

268 the transitions with large  $J$  slightly changed compared to the initial non-empirical CT  
 269 Hamiltonian due to the interactions with other sublevels.



270  
 271 **Figure 7.** The comparison of simulated and observed spectra of  $\text{CF}_4$  for  $T=113\text{ K}$  in the  
 272  $2169.8\text{--}2170.5\text{ cm}^{-1}$  region: calculated (red) spectra and  $\nu_1-2\nu_4\text{ (E)}$  (black); lower panel –  
 273 experimental (blue) spectra  $T=113\text{ K}$ .  
 274

275 Transitions of  $\nu_1 + 2\nu_4\text{ (E)}$  provide a noticeable absorption in the ranges  $2172\text{--}2173$   
 276  $\text{cm}^{-1}$  and  $2177\text{--}2180\text{ cm}^{-1}$ , but the transitions  $\nu_1 + 2\nu_4\text{ (F}_2\text{)}$  are also quite strong in both  
 277 ranges. The statistics of fitting the effective Hamiltonian are given in Table 4, and the  
 278 modified parameters of the effective Hamiltonian (compared to those initially computed from  
 279 the PES by contact transformations ) are given in Table 5.

280  
 281 Table 4. Information on the fit of EH to the experimental transitions

Band	RMS deviation * $10^{-3}$	Number of data	$J_{\text{max}}/J_{\text{min}}$
$\nu_1 + \nu_3$	1.195	284	20/4
$\nu_1 + 2\nu_4\text{ (F}_2\text{)}$	1.921	117	19/7

282  
 283 Table 5. Effective Hamiltonian parameters for the  $\nu_1 + \nu_3$  and  $\nu_1 + 2\nu_4$  bands.

Tensorial nomenclature			Parameter value
	Rotational	Vibrational	
1	R 0( 0, 0A1)	1010 1010	-1.0571136851E+01
2	R 1( 1, 0F1)	1010 1010	-7.3098294025E-03



3	R 2( 0, 0A1)	1010 1010	7.3935706176E-06
4	R 0( 0, 0A1)	1010 1002	4.8915047905E-01
5	R 0( 0, 0A1)	1002 1002	-2.7618876735E-01
6	R 1( 1, 0F1)	1002 1002	-4.6380494756E-03
7	R 2( 0, 0A1)	1002 1002	-3.9785009339E-04
8	R 2( 2, 0F2)	1002 1002	1.1713093142E-04

284

285

286

287

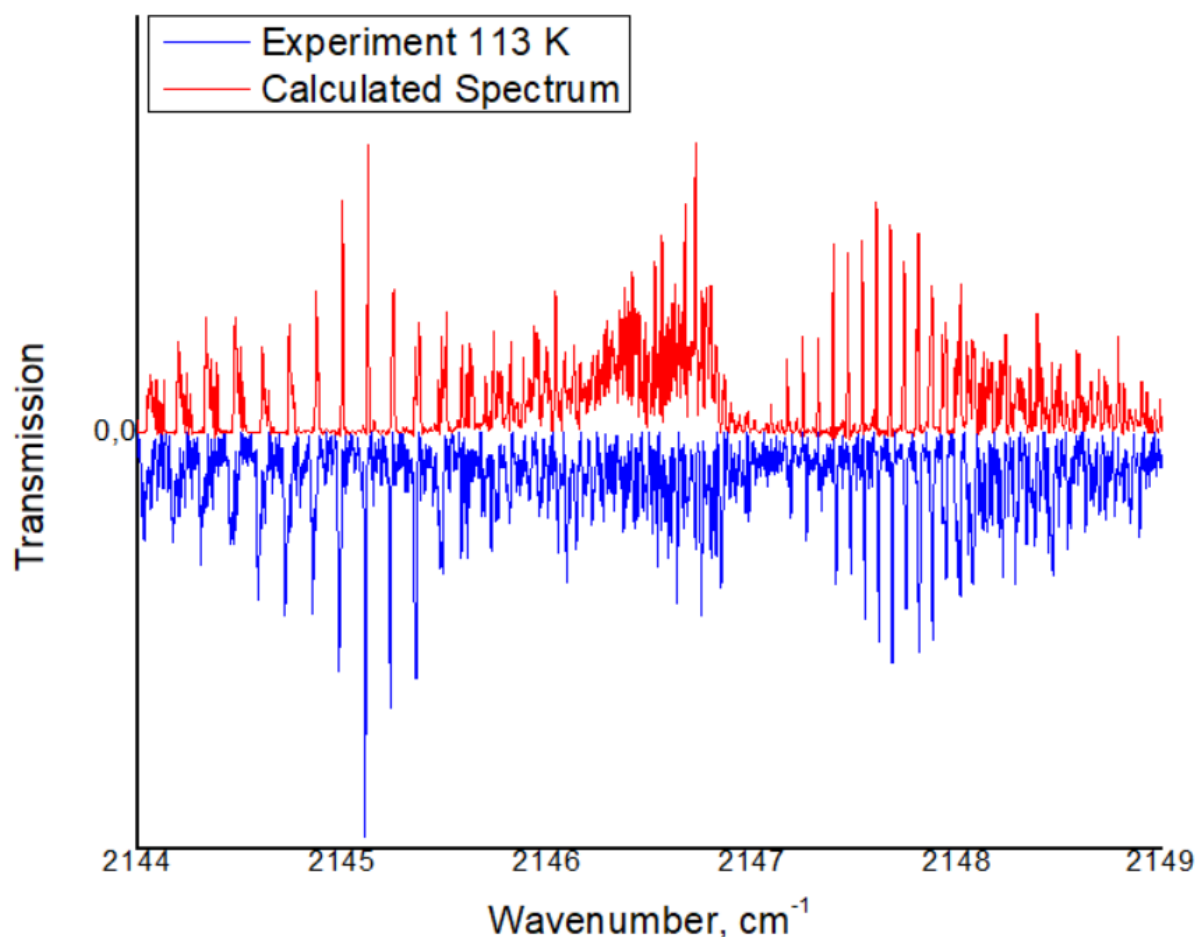
288

289

290

291

Another  $2\nu_2 + \nu_3$  band corresponding to three vibrational upper-state sublevels is visible in the  $2146\text{ cm}^{-1}$  region, see Figure 8. It is quite weak with more than 95% of absorption at 113 K due to transitions to the lower  $F_2$  vibrational sublevel at  $2147.34\text{ cm}^{-1}$ . This band was not analyzed. Variational calculations qualitatively well reproduce the spectrum, but slight distortions of the intensities were observed. No combinational differences for this band were found.



292

293

294

295

296

297

**Figure 8.** The comparison of simulated and observed spectra of  $\text{CF}_4$  for  $T=113\text{ K}$  in the  $2144. -2149. \text{ cm}^{-1}$  region: calculated (red) spectra of  $2\nu_2+\nu_3$  shifted by  $-0.13\text{ cm}^{-1}$ ; lower panel –experimental (blue) spectra  $T=113\text{ K}$ .

298 **Conclusion**

299 The main result of this work is the first high-resolution observation and analyses of the  
 300 infrared spectrum of CF<sub>4</sub> in the region of 2160–2210 cm<sup>-1</sup>. The strong  $\nu_1 + \nu_3$  band of this  
 301 range practically does not overlap with strong water lines and can be used for a remote  
 302 sensing of CF<sub>4</sub> in the atmosphere. For these purposes, a list of transitions was calculated with  
 303 noticeably more accurate line positions compared to initial ab initio based variational  
 304 calculations of [11]. An example of a computed list is shown in Table 6.

305  
 306

Table 6. An example of electronic supplementary data.

Key <sup>a</sup>	Position, cm <sup>-1</sup> <sub>b</sub>	Intensity, cm/molecule <sup>c</sup>	Rotational assignment <sup>d</sup>		K <sup>i</sup>	Vibrational assignment <sup>j</sup>	E <sub>lower</sub> , cm/molecule <sup>k</sup>
			Lower state	Upper state			
+	2169.300541	4.545e-24	0 7 F1 1	9 8 F2 64	K 0 1	1002F2	10.706588
+	2169.300601	5.347e-24	0 8 F2 2	9 9 F1 71	K 0 1	1002 F2	13.765624
+	2169.307311	3.545e-24	0 8 E 2	9 9 E 46	K 0 1	1002 F2	13.765619
+	2169.326621	5.174e-24	0 8 F1 2	9 9 F2 70	K 0 2	1002 F2	13.765603
+	2169.335560	2.258e-25	0 14 F2 3	9 14 F1 122	K 1 2	1002 E	40.148104
-	2171.228600	3.383e-24	0 11 F2 1	9 12 F1 93	K 0 2	1002 F2	25.236247

307 <sup>a</sup>"+" assigned line, "-" unassigned line.

308 <sup>b</sup>calculated line position.

309 <sup>c</sup>calculated line intensities at T = 296 K.

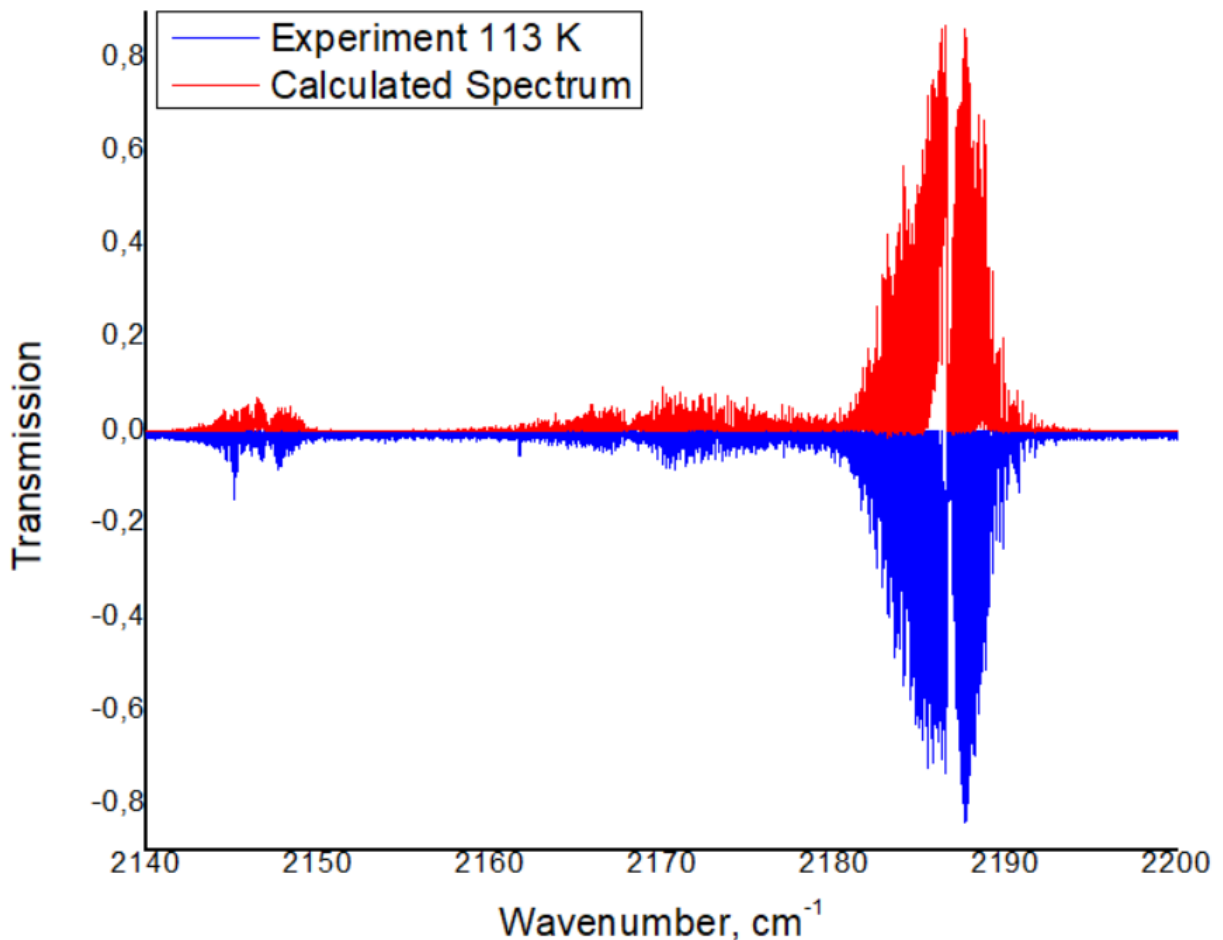
310 <sup>d</sup>rotational identification for bottom and top states.

311 <sup>i</sup>lower and upper rotational quantum number K .

312 <sup>j</sup>vibrational identification.

313 <sup>k</sup>calculated energy of the lower state.

314 The calculated list of lines was verified by comparison with high resolution  
 315 measurements at T = 113 K and T = 196 K. All results will be included in the TheoReTS  
 316 information system.



317  
 318 **Figure 8.** The comparison the simulations using our line list (red) with the experimental  
 319 spectrum of CF<sub>4</sub> (blue) at 113 K.  
 320

### 321 Acknowledgments

322 The authors acknowledge of RFBR grant (Grant No. 20-35-90075) is also acknowledged.  
 323

### 324 References

- [1] J. Harnisch, R. Borchers, P. Fabian, M. and Maiss, Tropospheric trends for CF<sub>4</sub> and C<sub>2</sub>F<sub>6</sub> since 1982 derived from SF<sub>6</sub> dated stratospheric air *Geophys. Res. Lett.* 23 (2000) 1099-1102.
- [2] J. Harnisch, Hohne N., Comparison of Emissions Estimates Derived from Atmospheric Measurements with National Estimates of HFCs, PFCs and SF<sub>6</sub> *Environ Sci Pollut Res* 9 (2002) 315-319.
- [3] J. Harnisch, D. Jager, J. Gale, O. Stobbe, Halogenated Compounds and Climate Change: Future Emission Levels and Reduction Costs *Environ Sci Pollut Res* 9 (2002) 369-374.
- [4] M.A. K. Khalil, R.A. Rasmussen, J.A. Culbertson, J.M. Prins, E.P. Grimsrud, M.J. Shearer, Atmospheric Perfluorocarbons *Environ. Sci. Technol.* 37 (2003) 4358 – 4361.
- [5] A.R. Ravishankara, S. Solomon, A.A. Turnipseed, R.F. Warren, "Atmospheric Lifetimes of Long-Lived Halogenated Species," *Science*, vol. 259, pp. 194 - 199, 1993.

- [6] R. Zander, S. Solomon, E. Mahicu, A. Goldman, C.R. Rinsland, M.R. Gunson, M.C. Abrams, A.Y. Chang, R.J. Salawitch, H.A. Michelsen, M.J. Newchurch, Stiller.G. P., Increase *Geophys. Res. Lett.* 23 (1996), no. 17 2353 — 2356.
- [7] V. Boudon, J.-P. Champion, T. Gabard, G. Pierre, M. Loete, C. Wenger, "Spectroscopic tools for remote sensing of greenhouse CH<sub>4</sub>, CF<sub>4</sub> and SF<sub>6</sub>," *Environ Chem. Lett.*, vol. 1, pp. 86 - 91, 2003.
- [8] T. Gabard, G. Pierre, M. Takami, "Study of the  $\nu_3$  and  $2\nu_4$  interacting states of  $^{12}\text{CF}_4$  ," *Mol. Phys.*, vol. 85, pp. 735–44, 1995.
- [9] V. Boudon, J. Mitchell, A. Domanskaya, C. Maul, R. Georges, A. Benidar, W.G. Harter, "High-resolution spectroscopy and analysis of the  $\nu_3/2\nu_4$  dyad of CF<sub>4</sub> ," *Mol. Phys.*, vol. 109, pp. 2273–90, 2011.
- [10] M. Carlos, O. Gruson, C. Richard, V. Boudon, M. Rotger, X. Thomas, C. Maul, C. Sydow, A. Domanskaya, R. Georges, P. Soulard, O. Pirali, M. Goubet, P. Asselin, T.R. Huet, *J. Quant. Spectrosc. Radiat. Transfer*, vol. 201, pp. 75 - 93, 2017.
- [11] M. Rey, I.S. Chizhmakova, A.V. Nikitin, V.G. Tyuterev, Understanding global infrared opacity and hot bands of greenhouse molecules with low vibrational modes from first-principles calculations: the case of CF<sub>4</sub> *Phys. Chem. Chem. Phys.* 20 (2018) 21008-21033.
- [12] L.S. Rothman, I.E. Gordon, Y. Babikov, A. Barbe, D.C. Benner, P.F. Bernath, M. Birk, L. Bizzocchi, V. Boudon, L.R. Brown, et al., "The HITRAN 2012 molecular spectroscopic database," *J. Quant. Spectrosc. Radiat. Transf.*, vol. 130, pp. 4 – 50, 2013.
- [13] I.E. Gordon, L.S. Rothman, C. Hill, R.V. Kochanov, Y. Tan, P.F. Bernath, M. Birk, V. Boudon, A. Campargue, K. Chance, et al., "The HITRAN 2016 molecular spectroscopic database," *J. Quant. Spectrosc. Radiat. Transf.*, vol. 203, pp. 3 – 69, 2017.
- [14] N. Jacquinet-Husson, L. Crepeau, R. Armante, C. Boutammine, A. Chédin, N. Scott, C. Crevoisier, V. Capelle, C. Boone, N. Poulet-Crovisier, et al., "The 2009 edition of the GEISA spectroscopic database," *J. Quant. Spectrosc. Radiat. Transf.*, vol. 112, pp. 2395 – 445, 2011.
- [15] N. Jacquinet-Husson, R. Armante, A. Scott, A. Chédin, L. Crépeau, C. Boutammine, A. Bouhdaoui, C. Crevoisier, V. Capelle, C. Boone, et al., "The 2015 edition of the GEISA spectroscopic database," *J. Mol. Spectrosc.*, vol. 327, pp. 31 – 72, 2016.
- [16] A.V. Nikitin, J.-P. Champion, V.I. Tyuterev, "The MIRS computer package for modeling the rovibrational spectra of polyatomic molecules," *J. Quant. Spectrosc. Radiat. Transfer.*, vol. 82, pp. 239 - 249, 2003.
- [17] A.V. Nikitin, M. Rey, J.-P. Champion, Tyuterev V.I. G., Extension of the MIRS computer package for modeling of molecular spectra: from effective to full ab initio rovibrational hamiltonians in irreducible tensor form *J. Quant. Spectrosc. Radiat. Transf.* 113 (2012) 1034–42.
- [18] B.I. Zhilinskii, V.I. Perevalov, V.I. Tyuterev, *Method of irreducible tensorial operators in the theory of molecular spectra*. Novosibirsk: Nauka, 1987.
- [19] J.-P. Champion, M. Loete, G. Pierre, *Spectroscopy of the earth's atmosphere and interstellar medium*, K.N. Rao and A. Weber, Eds. San Diego: Academic Press, 1992.
- [20] M. Mattoussi, M. Rey, M. Rotger, A.V. Nikitin, I. Chizhmakova, X. Thomas, H. Aroui, S. Tashkun, V.I. Tyuterev, Preliminary analysis of the interacting pentad bands ( $\nu_2 + 2\nu_4$ ,  $\nu_2 + \nu_3$ ,  $4\nu_2$ ,  $\nu_1 + 2\nu_2$ ,  $2\nu_1$ ) of CF<sub>4</sub> in the 1600–1800 cm<sup>-1</sup> region *J. Quant. Spectrosc. Radiat. Transfer* 226 (2019) 92 - 99.
- [21] V.I. Tyuterev, S.A. Tashkun, M. Rey, R.V. Kochanov, A.V. Nikitin, T. Delahaye,

- Accurate spectroscopic models for methane polyads derived from a potential energy surface using high-order contact transformations *J. Phys. Chem.* 117 (2013) 13779–805.
- [22] V.I.G. Tyuterev, S.A. Tashkun, H. Seghir, "High-order contact transformations: general algorithm, computer implementation, and triatomic tests," *SPIE*, vol. 5311, pp. 164 - 176, 2004.
- [23] V.G. Tyuterev, S. Tashkun, M Rey, A. Nikitin, High-order contact transformations of molecular Hamiltonians: general approach, fast computational algorithm and convergence of ro-vibrational polyad models *Molec. Phys.* 120 (2022) e2096140.
- [24] M Rey, Novel methodology for systematically constructing global effective models from ab initio-based surfaces: A new insight into high-resolution molecular spectra analysis *J. Chem. Phys* 292 (2022) 108349.
- [25] M. Rey, A.V. Nikitin, Y. Babikov, V.I.G. Tyuterev, TheoReTS – An information system for theoretical spectra based on variational predictions from molecular potential energy and dipole moment surfaces *J. Molec. Spectrosc.* 327 (2016) 138–158.
- [26] M. Rey, A.V. Nikitin, V.I.G. Tyuterev, "Ab initio ro-vibrational Hamiltonian in irreducible tensor formalism: a method for computing energy levels from potential energy surfaces for symmetric-top molecules," *Mol. Phys.*, vol. 108, pp. 2121-35, 2010.
- [27] A.V. Nikitin, O.M. Lyulin, S.N. Mikhailenko, V.I. Perevalov, N.N. Filipov, I.M. Grigoriev, I. Morino, T. Yokota, R. Kumazawa, T. Watanabe, GOSAT-2009 methane spectral line list in the 5550–6236 cm<sup>-1</sup> range. *J. Quant. Spectrosc. Radiat. Transfer* 111 (2010) 2211-2224.
- [28] A.V. Nikitin, O.M. Lyulin, S.N. Mikhailenko, V.I. Perevalov, N.N. Filippov, I.M. Grigoriev, I. Morino, Y. Yoshida, T. Matsunaga, GOSAT-2014 methane spectral line list *J. Quant. Spectrosc. Radiat. Transfer.* 154 (2015) 63–71.
- [29] V.I. Perevalov, V.I.G. Tyuterev, B.I. Zhilinskii, Ambiguity of spectroscopic parameters in the case of accidental vibration—rotation resonances in tetrahedral molecules. r<sub>2</sub>J and r<sub>2</sub>J<sub>2</sub> terms for E-F<sub>2</sub> interacting state *Chem. Phys. Lett.* 104 (1984) 455–61.
- [30] M Rey, A.V. Nikitin, B. Bézard, P. Rannou, A. Coustenis, V.G. Tyuterev, New accurate theoretical line lists of 12 CH<sub>4</sub> and 13 CH<sub>4</sub> in the 0–13400 cm<sup>-1</sup> range: Application to the modeling of methane absorption in Titan's atmosphere *Icarus* 303 (2018) 114-130.
- [31] V.I.G. Tyuterev, J.P. Champion, G. Pierre, V.I. Perevalov, "Fourth-order invariant parameters for F<sub>2</sub> isolated fundamental states of tetrahedral molecules: The study of the ν<sub>4</sub> band of 12CH<sub>4</sub>," *J. Mol. Spectrosc.*, vol. 105, pp. 113 - 138, 1984.